

Cobalt-doped β -peptide nanotubes: A class of spintronic materials

Biplab Sanyal and Olle Eriksson

Department of Physics, Uppsala University, P.O. Box 530, SE-751 21 Uppsala, Sweden

Per I. Arvidsson

*Department of Biochemistry and Organic Chemistry, Uppsala University, P.O. Box 576, SE-75123 Uppsala, Sweden
and Discovery CNS and Pain Control, AstraZeneca R&D Södertälje, SE-151 85 Södertälje, Sweden*

(Received 12 October 2007; published 4 April 2008)

We report a density functional theory based *ab initio* investigation of protein nanotubes formed by a stacking of β -peptide rings. We have optimized the structure of β -peptide rings arranged in a nanotube geometry. The calculated interatomic bond distances are found to agree with observations as is the equilibrium inter-ring separation. The electronic structure has been analyzed by calculating the density of states and band structures, which reveal wide band gap semiconducting properties of the tube. The possibility of doping β -PNT (peptide nanotube) with transition metal atoms is found to be energetically possible, and Co-doped β -PNT is found to be a strong ferromagnetic material, with relatively high ordering temperature and with impurity states just below the conduction band edge. This makes Co-doped β -PNT a very good potential candidate as an *n*-doped material in spintronics applications.

DOI: [10.1103/PhysRevB.77.155407](https://doi.org/10.1103/PhysRevB.77.155407)

PACS number(s): 75.75.+a, 71.15.Mb, 71.70.Gm, 73.22.-f

I. INTRODUCTION

Novel materials for use in spintronics applications are continuously sought after. The attention is caused by the potential of manipulating the electron spin in semiconducting devices, which may offer an improvement compared to conventional charge controlled devices. Currently, most of the attention is paid to diluted magnetic semiconductors (DMSs) for which applications in, e.g., nonvolatile memories and smaller electronic components have been suggested.^{1,2} The main goal which this research strives for is to develop a ferromagnetic semiconductor which is operational at room temperature. To realize this, it is necessary to identify a compound or an alloy with a magnetic ordering temperature well above room temperature and where at least one atomic species has a rather substantial magnetic moment. In addition, the material should have semiconducting properties. The main problem with DMS materials is that it has been shown to be difficult to synthesize a material which shows robust and undisputable magnetic properties. Instead, most materials which have been investigated have been reported to have either vanishing ferromagnetism or extremely high ordering temperatures in combination with low magnetic moments. The wide spread in properties is most likely connected to difficulties in controlling the crystal chemistry of the dopants (often *3d* elements), and it is not possible to rule out any of the conflicting experimental results.

In addition to DMS materials, other groups of materials are currently being investigated.³ For instance, organometallic molecular materials have recently been under focus. The conductivity of ferrocene-based molecular materials has, for instance, been both experimentally and theoretically investigated.⁴⁻⁶ These molecules contain transition metal atoms with unpaired spins, resulting in a molecular building block which naturally contains a magnetic moment. In addition, organometallic spintronics has been investigated in dicobaltocene switches,⁷ and a combination of correlated oxide materials and an organic semiconductor (sexithienyl)⁸ have

been experimentally investigated. In these spintronics materials encouraging results have been obtained. A large magnetoresistance found in these spintronic materials brings the hope for fabricating functional devices for the future. However, a problem with molecular electronics is connected to difficulties in controlling physical properties of single molecules in contact with Ohmic leads. Nevertheless, encouraging results have recently been demonstrated for the metallorganic porphyrine molecules on a Co or Ni substrate, where a superexchange mechanism was found to be responsible for the observed strong magnetic coupling between the molecule and the substrate.⁹

A class of materials which have potential in this field is peptide nanotubes (PNTs), and they are the focus of this paper. Here, the methodology we employ is theoretical, since all our results are based on density functional theory.¹⁰ However, it should be noted that such material specific calculations have been well established to reproduce electronic, structural, and magnetic properties of any material or molecule, with remarkable accuracy.¹¹

Let us now describe the host material of our study, namely, β -peptide based PNT (β -PNT). β -PNTs composed of β -amino-acid building blocks differ from those composed of α -amino-acids due to the special inherent ability of forming a parallel assembly of dipolar columns in which all amide groups of the PNT are oriented parallel to the tube axis; this generates a large dipole along the tube axis which may have a potential application to molecular devices. β -peptides actually have gained wider attention during the last couple of years predominantly due to a large variety of promising properties for applications in biomedical research.¹² However, β -peptides, especially cyclic analog,¹³ also show potential as building blocks for molecular nanowires fabricated by molecular self-assembly. Cyclic peptides are capable of stacking into peptide nanotubes through intermolecular hydrogen bonds between the rings.¹⁴ The size and length of such molecular nanowires are controllable by varying the ring size and side chains of the building blocks.¹⁵

β -peptides are composed of β -amino-acids instead of the α -amino-acids found in natural proteins. As such, these peptides contain one additional methylene group in their backbones, which render special properties to the peptide and allow substitutions to be placed at four desired three-dimensional positions, in contrast to the two stereochemically distinct positions present in normal α -peptides. A few *ab initio* calculations of peptide nanotubes exist. Carloni *et al.*¹⁶ studied the structural and electronic properties of octapeptide cyclo[-(D-Ala-Glu-D-Ala-Gln)₂] in the solid phase using plane wave based density functional theory¹⁰ calculations. They obtained a large gap (~ 4 eV) in the low-energy electronic excitation spectrum with the presence of extended and localized states near the gap. Okamoto *et al.*¹⁷ have previously theoretically studied the electronic conductivity of PNT composed of α -amino-acids of alternating chirality (a prerequisite for tubular stacking of peptides composed of α -amino-acids). They used the Hartree-Fock molecular orbital and density functional theories to study the electronic and molecular structures of PNTs.

II. COMPUTATIONAL DETAILS

In the present work, the theoretical calculations were performed using density functional theory as implemented in the Vienna *ab initio* simulation package (VASP)¹⁸ within the projector augmented wave method.¹⁹ The plane wave cut-off energy was set to be 450 eV. We have used both local density approximation (LDA)²⁰ as well as generalized gradient approximation (GGA)²¹ for the treatment of exchange-correlation functional.²² A periodic supercell having a lateral dimension of $15 \times 15 \times 15 \text{ \AA}^3$ was used with the molecule in the center of the cell. For the determination of the intermolecular separation, we varied the size of the cell in the z direction and calculated the total energies. Equilibrium geometry of the molecular and the intermolecular separations was determined by relaxing the atomic positions using the Hellmann-Feynman forces with a tolerance of 0.01 eV/\AA . We considered the Γ point only for the isolated molecule whereas a set of $2 \times 2 \times 3$ k points was used in the Monkhorst-Pack scheme²³ for the calculations of an infinite stacking of peptide rings. A Gaussian smearing method was used to calculate the density of states with a broadening parameter of 0.2 eV .

III. RESULTS

We start by comparing our theoretical results with existing experimental data of isolated peptide rings as well as for peptide nanotubes. We then proceed with discussing the main result of our study, namely, transition metal doped peptide nanotubes and their potential as spintronics materials.

A. Isolated peptide ring and undoped peptide nanotubes

An isolated peptide ring has 15 H, 9 C, 3 N, and 3 O atoms, as shown in Fig. 1. Starting from an experimental geometry,²⁴ we have relaxed the atomic positions in a ring and have calculated the ground state geometrical structure. The calculated bond distances of the equilibrium structure

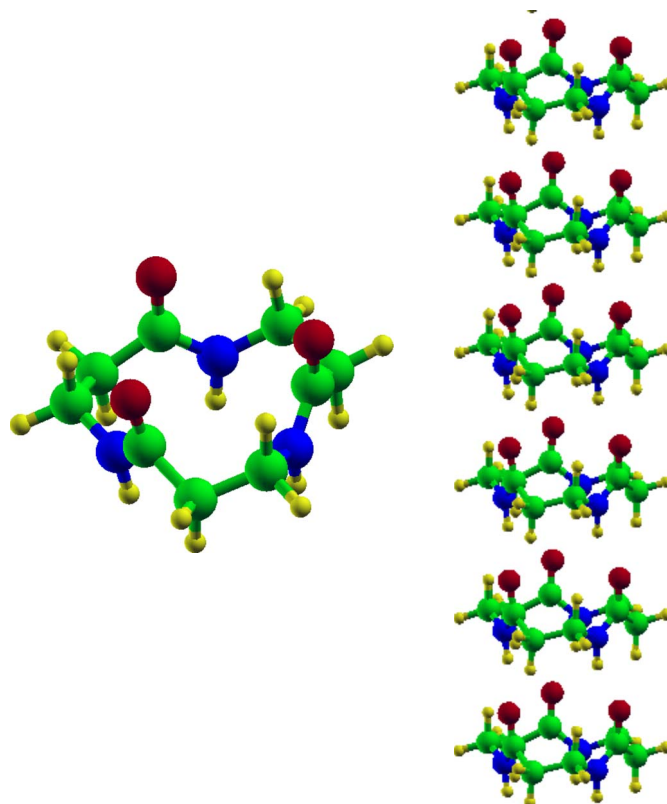


FIG. 1. (Color online) (Left) Structure of the isolated peptide ring; (right) the infinite stacking of rings. Red, blue, green, and yellow colors indicate O, C, N, and H atoms, respectively.

are given in Table I. It is clearly seen that the calculated average bond distances tally very well with the experimental ones.

Let us now proceed to discuss the results regarding β -PNTs formed by the stacking of peptide rings. In the β -PNT, the equilibrium inter-ring distance is dictated by the hydrogen bonding between the H and O atoms of two adjacent rings. In our calculation, we have varied the distance between adjacent rings and have calculated the total energies. In this case also, the atomic positions of the ring were relaxed for each inter-ring separation. We have used both LDA and GGA to calculate the equilibrium inter-ring distance. As is evident from Fig. 2, both methods give similar values of the position of minimum in the total energy curve. A closer inspection reveals that GGA is slightly better in determining the equilibrium separation as 4.8 \AA , which is in good agreement with experiment.²⁴ Therefore, we have adopted GGA for further calculations to be reported in the next sections.

TABLE I. Average bond distances between atoms for an isolated β -peptide ring. Both theoretical and experimental values (Ref. 24) are given. Different atoms are designated by their atomic symbols.

Bond distance (\AA)	C-O	N-H	C-C	C-N	C-H
Theory	1.23	1.02	1.51	1.36	1.11
Expt.	1.22	1.01	1.53	1.41	1.10

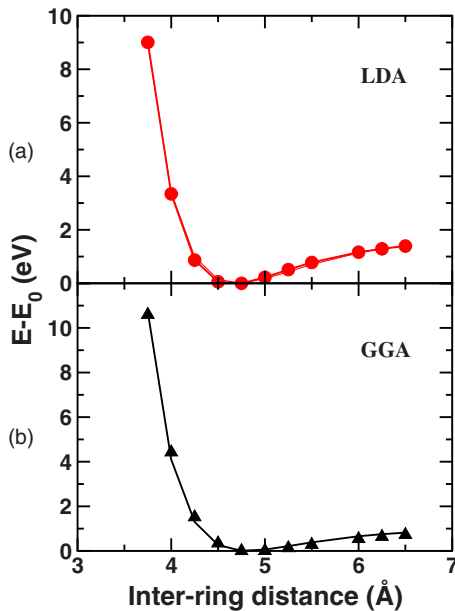


FIG. 2. (Color online) Total energy vs inter-ring separation for (a) LDA and (b) GGA exchange-correlation functionals. The solid curves are obtained by fitting the calculated values with a Morse function.

In Fig. 3, we show the band structure, density of states (DOS) of the β -PNT along with energy resolved charge densities. An inspection of Fig. 3(a) reveals that close to the highest occupied molecular orbital (HOMO) level, bands with $O p/N p$ character have some dispersion resulting in a small width in the DOS. However, two bands in this energy range (0 to -1 eV) show much less dispersion, signifying that the states are quite localized. In the energy range of 2–7 eV below the HOMO, the $C p$ DOS shows a broad feature with several bands with noticeable dispersion. In this energy range, $C p$ states mainly hybridize with $O p$ states along with $N p$ and $H s$ states. A significant energy gap of around 4 eV is present between the HOMO and lowest unoccupied molecular orbital (LUMO). The unoccupied part of the DOS around an energy span of 2 eV above LUMO is dominated by $C p$ states. There also, hybridization leads to a significant dispersion in the bands. This demonstrates that the lowest conduction band states can carry a current through the β -PNT, by electron hopping from one peptide ring to another, primarily via $C p$ states. Figure 3(a) shows that β -PNT should be characterized as a wide band semiconducting material.

The bonding properties of β -PNT are best illustrated from an energy resolved charge density. In Fig. 3(b), we hence show the isosurface charge density for states in an energy interval of -2 to -7 eV with respect to HOMO. It was mentioned above that for this energy interval, the dominant contributions in the DOS come from $C p$ and $O p$ states. From the charge density, one may observe that these two orbitals dominate the charge density plot. For HOMO [Fig. 3(c)], the $O p$ orbitals are primarily a combination of p_x and p_y types, resulting in density contours (and chemical bonds) mostly lying in the x - y plane. Finally, in Fig. 3(d), charge density for LUMO is shown. The presence of p states of C, O, and N is

prominent. The analysis for states of the occupied DOS establishes that the chemical bonding of β -PNT is best described as being covalent between atoms within one ring structure of a β -amino-acid group and a Coulomb attraction between negatively charged O atoms of one ring structure and the positively charged H atoms of the neighboring ring.

B. Transition metal doped peptide ring

The results mentioned above serve to demonstrate that the theoretical method is successful in reproducing the chemical bonding and electronic properties of this class of materials. We now proceed with an analysis of doping this material with transition metal atoms and the potential of using it as a spintronics material. Dopants were selected from the 3d transition metal series (Cr, Mn, Fe, and Co) and were introduced in a central position in β -PNT. The final position of each dopant was then determined by a total energy minimization, much in the same way as the calculations behind the results of Table I. The final positions of the dopants were found in all cases to be close to the O atoms of a β -amino-acid ring, in a centered position of β -PNT.

In Fig. 4, we show the calculated energy difference between ferromagnetically and antiferromagnetically coupled transition metal atoms in β -PNT. In order to achieve functionality of spintronics devices, it is important to have a ferromagnetic material,² preferably with an ordering temperature above room temperature. Hence, Fig. 4 shows that out of the selected group of dopants, Co stands out as the successful candidate. It should also be noted that the strength of the magnetic (exchange) coupling is quite strong since the calculated energy difference between ferromagnetic and antiferromagnetic couplings is 40 meV/atom. A mean field analysis,²⁵ which is appropriate in the present case of strong neighboring magnetic atoms, reveals an ordering temperature of 350 K, which demonstrates an ordering temperature above room temperature.

The trend exhibited in the stability of the ferromagnetic states has its counterpart in the transition metal doped CoAlO_2 system. This material was theoretically studied in Ref. 26. The trend is explained by the fact that the superexchange mechanism dominates in the early part of the 3d transition metal series, whereas for the later part, the double exchange mechanism dominates. The electronic structure shown in Fig. 6 shows that the d states are in the band gap and that the Fermi level cuts through both the spin-up and spin-down states. As discussed in connection to other spintronics materials,²⁷ the broadening of levels when atoms are ferromagnetically arranged lowers the total energy in this situation. The double exchange mechanism can hence be quite strong for Co-doped β -peptide.

Details of the magnetic state become clear by an inspection of the calculated magnetization density, which is shown in the spin density plot in Fig. 5 along with the geometrical positions of the Co atoms in the peptide nanotube. In Fig. 5, one may note that most of the spin density is located around the Co atom, which is expected, since the magnetic moment of Co is $1.13\mu_B/\text{atom}$, which is much bigger than the moment of any other atom in the material. However, some po-

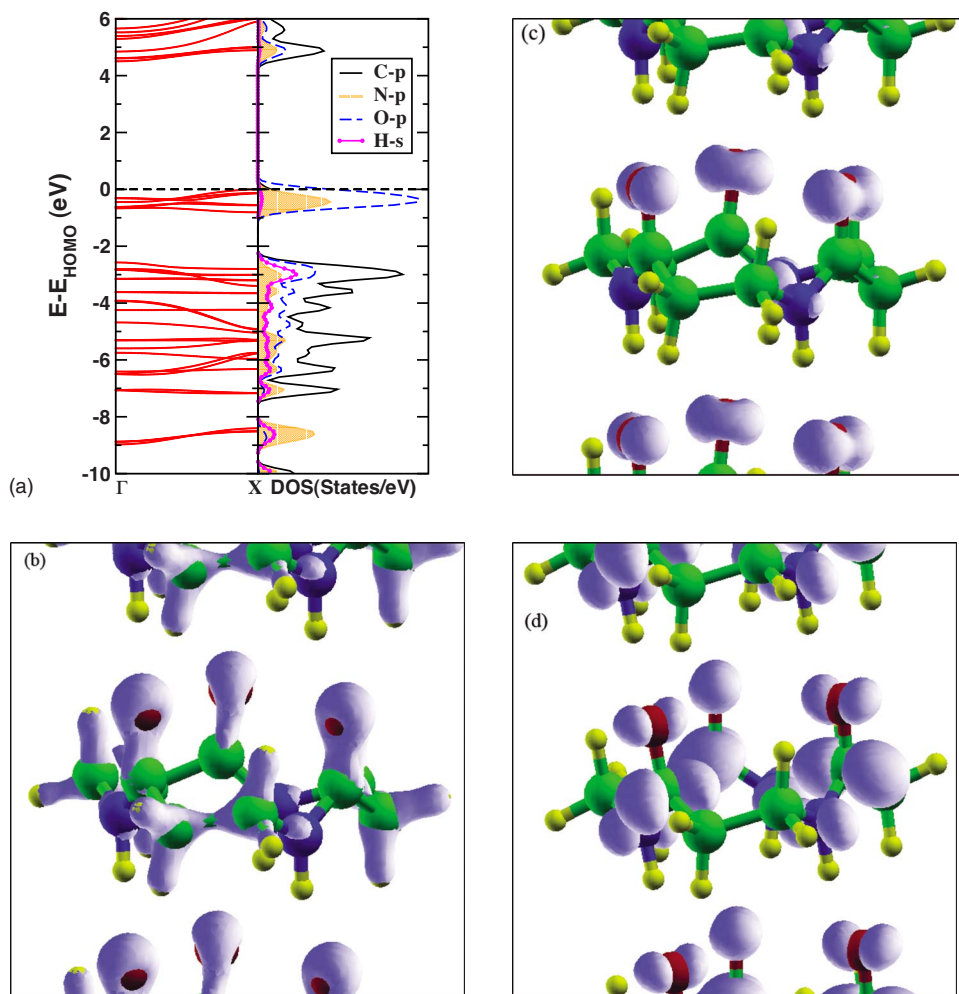


FIG. 3. (Color online) (a) Band structure along with the projected DOS of the infinite chain for an inter-ring separation of 4.8 Å. The dashed line corresponds to the HOMO, (b) isosurface charge density corresponding to an energy interval of -2 to -7 eV with respect to HOMO, (c) isosurface charge density for HOMO, and (d) same for LUMO.

larization is found also on the O atoms, which due to hybridization with Co d states pick up a moment of $0.02\mu_B$ /atom parallel to the moment on Co atom. The total magnetic moment of the unit cell with two Co atoms is $2.00\mu_B$, an integer value which is expected from the DOS. From the analysis of the projected charge and magnetic moment inside the Co

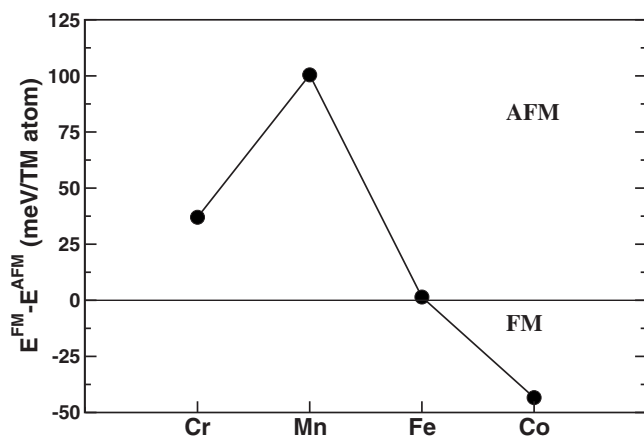


FIG. 4. Calculated energy difference between ferromagnetic and antiferromagnetic alignments of transition metal atoms in β -PNT. Values below zero indicate that ferromagnetism is preferable.

atomic spheres, one notes that Co has around four and three d electrons in the spin-up and spin-down channels, respectively, yielding a magnetic moment of about $1\mu_B$. The s - p state of a Co atom has around 0.8 electron in our calculation.

The calculated DOS of Co-doped β -PNT is shown in Fig. 6. Most of the structures of this DOS are similar to the DOS features shown for undoped β -PNT (Fig. 3), with a major exception being the Co derived states which are located in the band gap of β -PNT. It may be noted that donor states with a strong spin polarization, being derived from Co $3d$ orbitals, are found just below the conduction band edge of β -PNT. There is also some hybridization between the Co d states and the conduction band states, up to several eV above the conduction band edge. A close vicinity of the energies of the impurity states to the conduction band edge is the necessary criterion for a material to be used as an n -doped semiconducting devices. Although there is an energy gap between the Fermi level and the conduction band edge, the presence of small concentration of defects can easily push the impurity states close to the valence or conduction bands.²⁸ Furthermore, the fact that the dopant levels are strongly spin polarized, with an expected ordering temperature above room temperature, is the necessary criterion for materials to be used in spintronics devices. Hence, Fig. 6 shows evidence that for β -PNT doped with Co is a very promising candidate for spintronics materials.

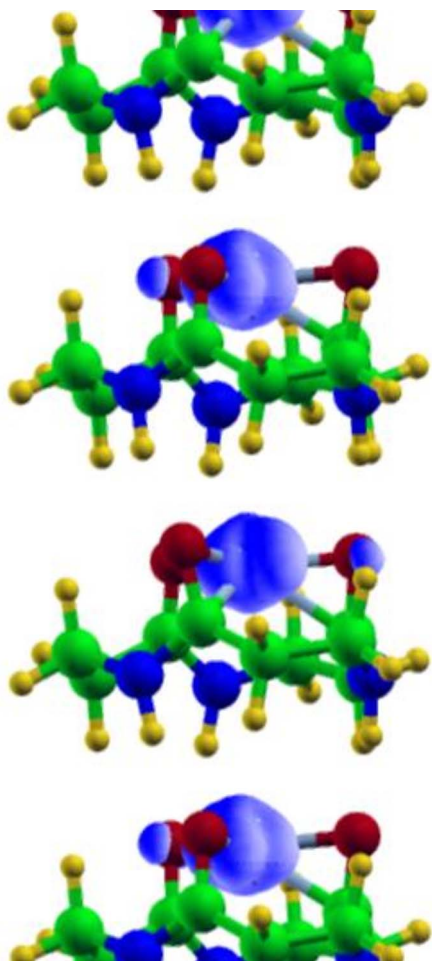


FIG. 5. (Color online) Calculated isosurface of the magnetization density of Co-doped β -PNT in the ferromagnetic alignment of the Co atoms.

Finally, we have calculated the formation energy of the impurity Co atom in the β -PNT host. The formation energy is defined as

$$E^{form} = E[\text{PNT} - \text{Co}] - (E[\text{PNT}] + E[\text{Co}]), \quad (1)$$

where $E[\text{PNT-Co}]$, $E[\text{PNT}]$, and $E[\text{Co}]$ are the total energies of the Co-doped β -PNT, undoped β -PNT, and metallic Co, respectively. The calculated formation energy is around 3 eV signifying the fact that the energy cost of creating Co impurities in β -PNT is similar to the energy cost of impurity doping of conventional semiconducting materials.²⁹ Hence,

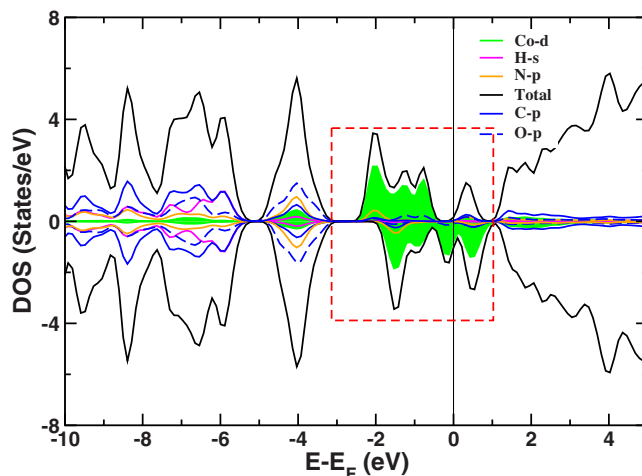


FIG. 6. (Color online) Calculated DOS of Co-doped β -PNT. The Co d states are marked in green. The states associated with the Co doping are found in the band gap of the β -PNT and are marked by a rectangular dashed frame.

the energetics of the presently suggested spintronics material is not prohibitive for its successful synthesis.

IV. CONCLUSION

In conclusion, we have investigated the electronic structure and chemical binding of β -peptide nanotubes, with and without Co doping. The optimized geometry of undoped β -PNT compares well with the experimental structure, both concerning bond distances of atoms within a peptide ring as well as the inter-ring distance (4.8 Å). β -PNT is further found to be a wide band semiconductor, with an energy gap of 4 eV. The possibility of doping β -PNT with transition metal atoms is found from the theory to be energetically possible, and Co-doped β -PNT is argued from the theoretical calculations to be a strong ferromagnetic material, with relatively high ordering temperature (above room temperature) and with impurity states just below the conduction band edge. This makes Co-doped β -PNT a very good potential as an n -doped material in spintronics applications.

ACKNOWLEDGMENTS

We acknowledge computational support from Swedish National Infrastructure for Computing (SNIC). We also wish to acknowledge support from the Swedish Research Council (VR) and the Foundation for Strategic Research (SSF).

¹G. Prinz, *Science* **282**, 1660 (1998).

²S. A. Wolf, D. D. Awschalom, R. A. Buhrman, J. M. Daughton, S. von Molnar, M. L. Roukes, A. Y. Chtchelkanova, and D. M. Treger, *Science* **294**, 1488 (2001).

³For a review on spintronics based on organic materials, see W. J. M. Naber, S. Faez, and W. G. van der Wiel, *J. Phys. D* **40**, R205

(2007).

⁴J. A. M. Dinglasan, M. Bailey, J. B. Park, and Al-Amin Dhirani, *J. Am. Chem. Soc.* **126**, 6491 (2004).

⁵S. A. Getty, C. Engtrakul, L. Wang, R. Liu, San-Huang Ke, H. U. Baranger, W. Yang, M. S. Fuhrer, and L. R. Sita, *Phys. Rev. B* **71**, 241401(R) (2005).

- ⁶C. Engtrakul and L. R. Sita, *Nano Lett.* **1**, 541 (2001).
- ⁷R. Liu, San-Huang Ke, H. U. Baranger, and W. Yang, *Nano Lett.* **5**, 1959 (2005).
- ⁸C. Taliani, V. Dediu, F. Biscarini, M. Cavallini, M. Murgia, G. Ruani, and P. Nozar, *Phase Transitions* **75**, 1049 (2002).
- ⁹H. Wende, M. Bernien, J. Luo, C. Sorg, N. Ponpandian, J. Kurde, J. Miguel, M. Piantek, X. Xu, Ph. Eckhold, W. Kuch, K. Baberschke, P. M. Panchmatia, B. Sanyal, P. M. Oppeneer, and O. Eriksson, *Nat. Mater.* **6**, 516 (2007).
- ¹⁰P. Hohenberg and W. Kohn, *Phys. Rev.* **136**, B864 (1964); W. Kohn and L. J. Sham, *ibid.* **140**, A1133 (1965).
- ¹¹O. Eriksson, *Encyclopedia of Materials: Science and Technology* (Elsevier, Amsterdam, 2006), pp. 1–11.
- ¹²For reviews, see C. M. Goodman, S. Choi, S. Shandler, and W. F. DeGrado, *Nat. Chem. Biol.* **3**, 252 (2007); D. Seebach, A. K. Beck, and D. J. Bierbaum, *Chem. Biodiv.* **1**, 1111 (2004).
- ¹³D. Seebach, J. L. Matthews, A. Meden, T. Wessels, C. Baerlocher, and L. B. McCusker, *Helv. Chim. Acta* **80**, 173 (1997); J. L. Matthews, K. Gademann, B. Jaun, and D. Seebach, *J. Chem. Soc., Perkin Trans. 1*, 3331 (1998); T. D. Clark, L. K. Buehler, and M. R. Ghadiri, *J. Am. Chem. Soc.* **120**, 651 (1998); B. Jagannadh, M. S. Reddy, C. L. Rao, A. Prabhakar, B. Jagadeesh, and S. Chandrasekhar, *Chem. Commun. (Cambridge)* 2006, 4847.
- ¹⁴M. R. Ghadiri, J. R. Granja, R. A. Milligan, D. E. McRee, and N. Khazanovich, *Nature (London)* **366**, 324 (1993); M. R. Ghadiri, J. R. Granja, and L. K. Buehler, *ibid.* **369**, 301 (1994); D. T. Bong, T. Dennis, T. D. Clark, J. R. Granja, and M. R. Ghadiri, *Angew. Chem., Int. Ed.* **40**, 988 (2001); S. W. Horne, N. Ashkenasy, and R. M. Ghadiri, *Chem.-Eur. J.* **11**, 1137 (2005); N. Ashkenasy, S. W. Horne, and R. M. Ghadiri, *Small* **2**, 99 (2006).
- ¹⁵X. Gao and H. Matsui, *Adv. Mater. (Weinheim, Ger.)* **17**, 2037 (2005); M. Reches and E. Gazit, *Curr. Nanosci.* **2**, 105 (2006); Yong Zhou, *Nanotechnology* **1**, 21 (2007).
- ¹⁶P. Carloni, W. Andreoni, and M. Parrinello, *Phys. Rev. Lett.* **79**, 761 (1997).
- ¹⁷H. Okamoto, K. Takeda, and K. Shiraiishi, *Phys. Rev. B* **64**, 115425 (2001).
- ¹⁸G. Kresse and J. Hafner, *Phys. Rev. B* **47**, 558 (1993); G. Kresse and J. Furthmüller, *ibid.* **54**, 11169 (1996).
- ¹⁹P. E. Blöchl, *Phys. Rev. B* **50**, 17953 (1994).
- ²⁰D. M. Ceperley and B. J. Alder, *Phys. Rev. Lett.* **45**, 566 (1980).
- ²¹J. P. Perdew and Y. Wang, *Phys. Rev. B* **45**, 13244 (1992).
- ²²R. M. Dreizler and E. K. U. Gross, *Density Functional Theory* (Springer-Verlag, Berlin, 1990).
- ²³H. J. Monkhorst and J. D. Pack, *Phys. Rev. B* **13**, 5188 (1976).
- ²⁴V. Tereshko, J. M. Monserrat, J. Perez-Folch, J. Aymami, I. Fita, and J. A. Subirana, *Acta Crystallogr., Sect. B: Struct. Sci.* **B50**, 243 (1994).
- ²⁵P. Mohn, *Magnetism in the Solid State: An Introduction* (Springer, Berlin, 2003).
- ²⁶H. Kizaki, K. Sato, and H. Katayama-Yoshida, *Jpn. J. Appl. Phys., Part 1* **44**, 1187 (2005).
- ²⁷H. Akai, *Phys. Rev. Lett.* **81**, 3002 (1998).
- ²⁸D. M. Iușan, B. Sanyal, and O. Eriksson, *Phys. Rev. B* **74**, 235208 (2006).
- ²⁹S. C. Erwin and A. G. Petukhov, *Phys. Rev. Lett.* **89**, 227201 (2002).